Hajian, Hatef; Ahmed, Kaiser; Kurnitski, Jarek

Dynamic heating control measured and simulated effects on power reduction, energy and indoor air temperature in an old apartment building with district heating

Published in:
Energy and Buildings

DOI:
10.1016/j.enbuild.2022.112174

Published: 01/08/2022

Document Version
Publisher's PDF, also known as Version of record

Energy & Buildings 268 (2022) 112174

Contents lists available at ScienceDirect

Energy & Buildings

journal homepage: www.elsevier.com/locate/enb

Dynamic heating control measured and simulated effects on power reduction, energy and indoor air temperature in an old apartment building with district heating

Hatef Hajian [a,*], Kaiser Ahmed [a], Jarek Kurnitski [a,b]

[a] Department of Civil Engineering, Aalto University, 02150 Espoo, Finland
[b] FinEst Centre for Smart Cities (Finest Centre), Tallinn University of Technology, 19086 Tallinn, Estonia

ARTICLE INFO

Article history:
Received 26 March 2022
Revised 26 April 2022
Accepted 11 May 2022
Available online 13 May 2022

Keywords:
Space heating
Heating power
Power reduction
Heating curve
Dynamic control
Central heating

ABSTRACT

This study investigated the effects of the dynamic heating control on power reduction and indoor air temperature in a typical Finnish block of apartments built in 1981. The building operated in 2018 with conventional and in 2020 with dynamic heating control. The onsite measured data was collected from both periods. Measured data enabled calibrating the whole building simulation models with an accuracy better than 10%. A new dynamic heating curve control algorithm was developed so that outdoor air compensated supply temperature was reduced during high use of Domestic Hot Water (DHW) by applying DHW compensation differential. If the indoor air temperature in any apartment dropped below the limit, supply temperature uplift was applied. The dynamic heating control resulted in 8.9% space heating and 13.7% total heating power reduction while had practically no effect on energy use. On the contrary, dynamic heating control slightly increased indoor temperature fluctuations, but both control systems resulted in a similar value of hours below the setpoint temperature of 21 °C. The results demonstrate that heating power reduction without compromising indoor air temperature is possible with applied supply temperature drop during DHW peaks and preheating afterwards.

1. Introduction

Building energy demand has become a significant part of global energy usage as the world's population and economy have grown [1]. According to IEA & UNEP (2018), construction and operations of buildings contributed to 36% of worldwide total energy use and 39% of Greenhouse Gas (GHG) emission attributable to energy in 2017 [2]. In the European Union (EU), buildings accounted for 40% of energy usage and 36% of GHG emissions [3]. Across the EU, the most energy-efficient dwellings are found in Austria, Ireland, Finland, and Sweden [4]. Correspondingly in Finland, dwellings contributed to 20% of total energy use on average [5]. On the other hand, buildings have the potential to provide significant energy savings during the design, construction, and operation phases [6]. It is estimated that validated and commercially viable technologies can cut building energy use by 30% to 80% in developed and developing countries, resulting in significant reductions in GHG emissions [7].

In Finland, residential building Space Heating (SH) accounted for almost 68%, Domestic Hot Water (DHW) heating 15%, appliances 12%, and saunas heating 5% of household energy usage [5]. Most Finnish apartment buildings have a central heating system and are connected to the District Heating (DH) [8]. Heating systems are controlled with outdoor air compensated Heating Curve (HC), and the maximum supply water temperature at the design outdoor temperature (−26 °C in Helsinki) is typically 70 °C in existing building stock [9]. There is a great interest in improving the energy performance of buildings and among many possible measures, improved heating control so that overheating and wasteful energy use can be avoided is often discussed. Benakopoulos et al. (2019) showed that operating the building SH system with high flow and low supply temperature can provide a low-cost, energy-efficient solution [10]. Likewise, Tunzi et al. (2016) claimed cheaper end-user energy bills by utilizing low return temperature in existing buildings [11]. However, to ensure saving energy, radiator heat output and the system balancing and control with Thermostatic Radiator Valves (TRVs) must be carefully considered [12].

Various terms for dynamic heating control system are reported in the literature, namely 'adaptive control', 'demand responsive control', 'adaptive heat curve', 'adaptive supply temperature

* Corresponding author.
E-mail addresses: hatef.hajian@aalto.fi (H. Hajian), kaiser.ahmed@aalto.fi (K. Ahmed), jarek.kurnitski@taltech.ee (J. Kurnitski).

https://doi.org/10.1016/j.enbuild.2022.112174
0378-7788/

control', etc. According to Saloky et al. (2005), adaptive control is one solution to avoid inaccurate desirable heating system measures as the control system's parameters vary over time [13]. Xu et al. (2011) suggested an adaptive control strategy in which the system's heat supply quantity varies in response to changes in the heat load, and the system's flow rate is maintained within a reasonable range [14]. They found that if the overheating is due to a high supply water temperature or a large radiator area, the TRV's efficiency can be as high as 80%. In the case of central air handling units, Elkhuizen et al. (2003) claimed that without having massive financial contributions, energy savings of up to 35% could be achieved by considering advanced heating control solutions without sacrificing thermal comfort in both new and existing buildings [15,16]. Building residents may experience discomfort, productivity loss, and health problems as a result of overheating [17]. In addition, according to the outcomes of a survey conducted by Bruce-Konuah et al. (2018), householders in UK social housing prefer cooler thermal condition [18]. Therefore, Sun et al. (2021) suggested a dynamic heating strategy relying on online prediction and indoor temperature feedback, which successfully moderated overheating and saved about 6% of heating energy [19]. A similar result is by Ionesi et al. (2015) applying a heating curve based on an online structural and parametric learning method, which resulted in improved thermal comfort and a 5% reduction in energy use [20]. Unlike these studies reporting 5–6% saving, Hajian et al. (2021) showed, based on measured data in a typical Finnish apartment building for 1970–1980, that lowering the SH supply water temperature and saving energy was not possible since the indoor air temperature was immediately compromised [21]. This indicates that there are many old buildings where easy saving potentials are not untapped but already taken into use by heating curve adjustments, use of thermostats and adequate balancing and maintenance of the heating system.

However, it is worth studying would the application of dynamic heating control enable saving energy and minimize heating power without sacrificing indoor air temperature. By implementing dynamic heating control, some service providers promise considerable energy savings and power reduction with a good indoor climate. For example, a commercial dynamic heating control system claims that the typical building's energy cost descends between 10% and 20% [22]. Therefore, there is a clear research gap in buildings where easy energy saving potentials are taken into use, would the dynamic heating control systems enable heating power reduction while not compromising indoor air temperature, as no studies have looked at the possible peak power reductions in such buildings. Formalizing control algorithms and testing their performance in real buildings would allow to understand their application potential and impacts on energy efficiency improvement.

Most people spend 90% of their time indoors and are dependent on mechanical heating systems and air conditioning [6]. Proper indoor temperature is essential for occupant thermal comfort and drives energy usage in relation to outdoor weather conditions through space heating and cooling [23]. A study of buildings with the conventional heating control system in the UK discovered that a rise of 10% in indoor air temperature led to a 15% increase in heating energy [24]. However, the relation is not linear because heat gains compensate for a considerable part of heat losses [22–24]; still, it is clear that even small changes in indoor air temperature led to considerable energy effects.

This study was initiated to evaluate experimentally and by simulations the potential of energy-saving and heating power reduction by implementing the dynamic heating control system in two typical 4-story apartment buildings in Helsinki, Finland, built in 1981. It was followed that heating control would not compromise indoor air temperature. Heating was controlled in the first measurement period in 2018 by the conventional system and after intervention by the dynamic heating control system in 2020. Onsite measured data was collected from both periods, and the IDA Indoor Climate and Energy (IDA ICE) simulation tool was used for model calibration and energy and indoor climate simulation. Both conventional and dynamic heating control models were calibrated against the onsite measured data with acceptable accuracy. Indoor temperature setpoints were assessed from room temperature measured data, and computing the mean yearly hours' length of deviation of indoor air temperature at the apartment and building level enabled exact comparison of control systems at the same indoor air temperature. The dynamic heating control model was developed and implemented so that the outdoor temperature compensated heating curve was modified based on minimum room temperature among all apartments and the DHW flow rates. This allowed benchmarking both heating energy use and heating power reduction for space and domestic hot water.

2. Methodology

2.1. Building characteristics

The case study building representing a typical Finnish non-renovated multifamily apartment building was constructed in 1981 and located in Helsinki. It consists of two 4-story concrete blocks of apartments (A and B), as shown in Fig. 1. Building A includes 22 apartments, three staircases and two common rooms, whereas building B has 16 apartments, two staircases and one common room. The total number of occupants is 104 persons. The overall heated area in both buildings was 4085.8 m^2. The building envelope heat transmittance coefficient (U-value) and area are shown in Table 1. The windows were kept as they were; therefore, the 3-pane glazing had no low emission layer, which explains their high U-value. The windows Solar Heat Gain Coefficient value (SHGC) was 0.68. Moreover, the window-wall ratio was 29.3% in buildings A and B.

Both buildings were ventilated via a mechanical exhaust ventilation system. The airflow rate of fans was 0.29 l/(s m^2) and 0.45 l/(s m^2) in heating and summer seasons, respectively, which was determined in our model calibration procedure reported with a tabulated fan operation schedule in [21].

The modelled SH system comprised 600 mm high water radiators of type 11 with output heat of 1018 W/m at 70/40/21 °C and 2 K dead-band proportional thermostats. In the calibration with dynamic heating control onsite measured data, the radiator oversizing of 15% was assumed. The designed outdoor temperature was −26 °C.

Fig. 1. The case study building with A and B blocks.

Table 1
Building element characteristics.

Building element	Components (from inside to outside)	U-value, W/(m^2K)	Area, m^2
External wall	Concrete (600 mm)Mineral wool (120 mm)Concrete (100 mm)	0.34	2552.2
Roof	Lightweight concrete (600 mm) Insulation (300 mm)Lightweight concrete (200 mm)	0.29	1114.1
External floor	Plastic mat (5 mm)Lightweight concrete (20 mm)Concrete (200 mm)Cellular plastic sheet (120 mm)	0.29	1173.7
Glazing	3 pane glazing (4–12-4–12-4)	2.1	362.1

The buildings' leakage rate was determined to be approximately 4 m3/(h.m2 ext. surf.) at a 50 PA pressure difference. Data for infiltration airflow simulation, including wind speed and semi-exposed pressure coefficients, were implemented from a local weather station in the Finnish meteorological institute [25] and the Air Infiltration and Ventilation Centre (AIVC) [26], respectively.

The internal heat gain profiles (occupancy, appliances, and lighting) were specified based on ISO 17772-1:2017 [27] and are reported in detail in [21]. According to the Finnish building code [28], the appliances power is 4 W/m^2. Based on household electricity measurement data, this was raised to 4.4 W/m^2 during the model calibration process. Moreover, in cold months (Jan. to Mar. and Oct. to Dec.), the additional appliance profile was used as 1 W/m^2 to follow the metered patterns.

District heating measured data was used, but to simulate the DHW fluctuations realistically, the DHW profile shown in Fig. 2 was constructed with Ahmed et al. (2016) method based on the DHW consumption (l/person/day) and the number of occupants [29].

The available onsite measured data included hourly data of the total DH usage, electricity consumption (facility and apartments measured separately), and monthly Domestic Cold Water (DCW) usage. Our model calibration study reports the calculation of DHW energy use and circulation losses [21].

2.2. Research procedure

This research was designed to compare heating energy and power with a conventional and dynamic heating control at the same indoor air temperature. The building heating control system operated conventionally during 2018. After that, the dynamic control system was installed and operated in 2020. In the conventional heating control, onsite measured data was for full 2018, but in the dynamic heating control, this was limited to March 2020. The Autodesk Revit 2018 [30] software was used to model the building's geometry. Later on, the generated Industry Foundation Classes (IFC) file was imported to the Building Performance Simulation (BPS) [31] simulation tool IDA ICE [32] to run the energy simulation with apartment and staircase level zoning. Floor 3 in building A and floor 2 in building B were erased to lighten the simulation model. Hence, a multiplier of 2 was employed on the remained similar floors to keep the model characteristics the same with no effect on the model accuracy, as shown in Fig. 3.

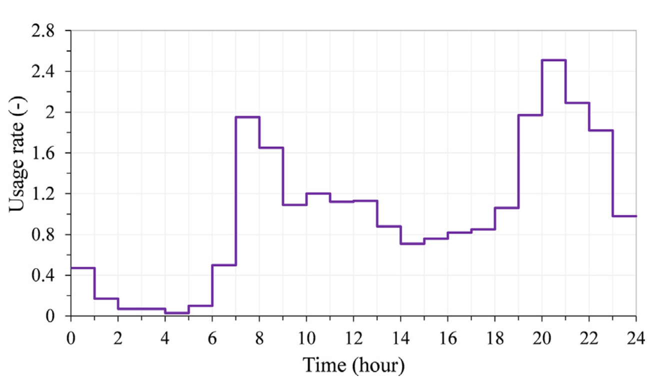

Fig. 2. The hourly DHW usage profile, according to Ahmed et al. [29].

In the model validation (index of agreement and coefficient of variation of the root mean square error), the simulation model was calibrated against the measured data. Subsequently, energy usage and indoor air temperature when the conventional heating control system operated during 2018 were assessed in [21].

The next step was to implement the dynamic heating control system into the conventional calibrated model. The dynamic control model was successfully recalibrated against the onsite measured data in March 2020, addressing the slightly higher apartments' measured electricity use than during the conventional heating control period in 2018. Finally, heating energy, heating power, and the indoor air temperature in the dynamic control simulation model were evaluated and compared with the conventional model results for which yearly simulation with 2020 weather data was conducted.

2.3. Conventional and dynamic heating control system

The existing conventional heating control system worked with the outdoor air temperature compensated heating curve 70/40 °C that was implemented in the conventional simulation model. For that purpose, the ideal heating curve was calculated for panel radiators of type 11 with a heat output of 1018 W/m at 70/40/21 °C and the radiator exponent value of 1.31. Fig. 4a shows how the outdoor air temperature compensated heating curve (solid line) is depicted with a second-order polynomial (dotted line) used in the simulation to define the heating curve. In the conventional heating control model, the room setpoint temperature was considered as 21 °C (in good agreement with measured temperatures), while in the dynamic heating control model, to ensure an equal indoor air temperature, the setpoints between 21 °C and 23 °C were tested. Finally, the dynamic control was tuned so that the same setpoint temperature of 21 °C was possible to use, leading to maximum power saving while maintaining the same indoor air temperature. Fig. 4b presents the heating curve when the dynamic equations were in operation in 2020. The minimum outdoor temperature in 2018 and 2020 was −26 °C and −8 °C, respectively, which explains the difference in outdoor temperature axis limits in Fig. 4a and 4b. The developed dynamic heating control algorithm and equations are explained in section 3.1.

The implemented dynamic heating control system consists of the new controller TC_1 that replaced the old one, as shown in Fig. 5. TC_1 regulates the SH supply water flow rate to keep the supply temperature. The supply temperature is recalculated from the conventional heating curve according to three criteria as reported in section 3.4:

1. The minimum indoor air temperature among all zones (T_{min}), which is measured with Temperature Sensors 1 in each apartment (TE_{1A},TE_{1B}, TE_{1C}) so that the space heating compensation temperature ($T_{SH,\,CT}$) ascends the supply temperature by 5 °C, if T_{min} drops below 19.5 °C in any apartment;
2. The HC supply temperature (T_{HC}) that is dependent on the outdoor temperature (T_o) measured with TE_2;

Fig. 3. IDA ICE simulation model.

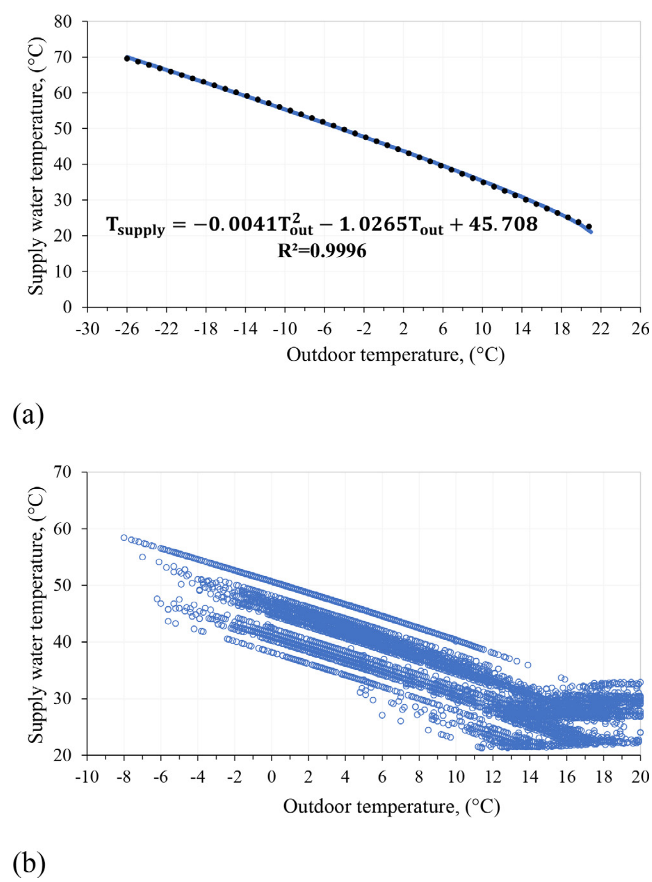

Fig. 4. Heating curve a) conventional control (2018), b) dynamic control in operation (2020).

3. The DHW compensation temperature ($T_{DHW, CT}$) reduction was specified via the DHW flow rate of Temperature Controller 2 (TC_2) so that at high DHW flow rates, the space heating supply temperature is reduced.

2.4. Model validation and accuracy

Assessing the simulated model performance by comparing the simulated data with measured data is the key task for any modelling analysis [30]. The index of agreement (d) and the Coefficient of Variation of the Root Mean Square Error (CVRMSE) were utilized in this study to evaluate the simulation model. The d value is acceptable if it is between 0 and 1 (0 < d < 1), and it was calculated as 0.9973 in this study. Besides, the CVRMSE value of less than 15% leads to acceptable model performance, calculated as 8.94% in this study. Furthermore, Sensitivity Analysis (SA) aims to determine the correctness of a given model specification and assess the reliability of the model's assumptions has been studied. Since there was no heat recovery, outcomes demonstrate good utilization of circulation heat loss and reasonable sensitivity to the airflow rate. The procedure used is reported in detail in [21].

2.5. Indoor air temperature assessment

To evaluate indoor air temperature conditions, the mean and operative air temperatures were analyzed at the individual apartment and building levels. According to the Indoor climate and ventilation of buildings in Finland [33], the room air temperature design value during the heating season is set as 21 °C. Similarly, based on standard TR16798-2:2019 [34] Table B.2, category II design operative air temperature value in winter is recommended as 20 °C.

The yearly air temperature deviation is admitted in estimating apartments overheating and underheating conditions [32]. Table E.1 in [29] shows that the length of deviation of a variable (yearly mean indoor air temperature) is calculated by dividing the number of hours in which the mean indoor air temperature is below 21 °C by the annual number of hours (8760 h). If the deviation length of mean indoor air temperature yearly hours stays below 6%, the indoor air temperature condition is met. The indoor air and operative temperature deviation were evaluated in this study based on the <6% value in the single apartment and building level.

Since the Finnish climate is heating-dominated, and the entire purpose of the study was to evaluate the impact of the dynamic control of the heating system, the indoor air temperature above 23 °C was not studied and presented while the space heating system was off.

3. Results and analysis

3.1. The dynamic heating control algorithm

As explained in section 2.3, the dynamic supply temperature ($T_{Dyn. sup.}$) algorithm was developed based on three parameters.

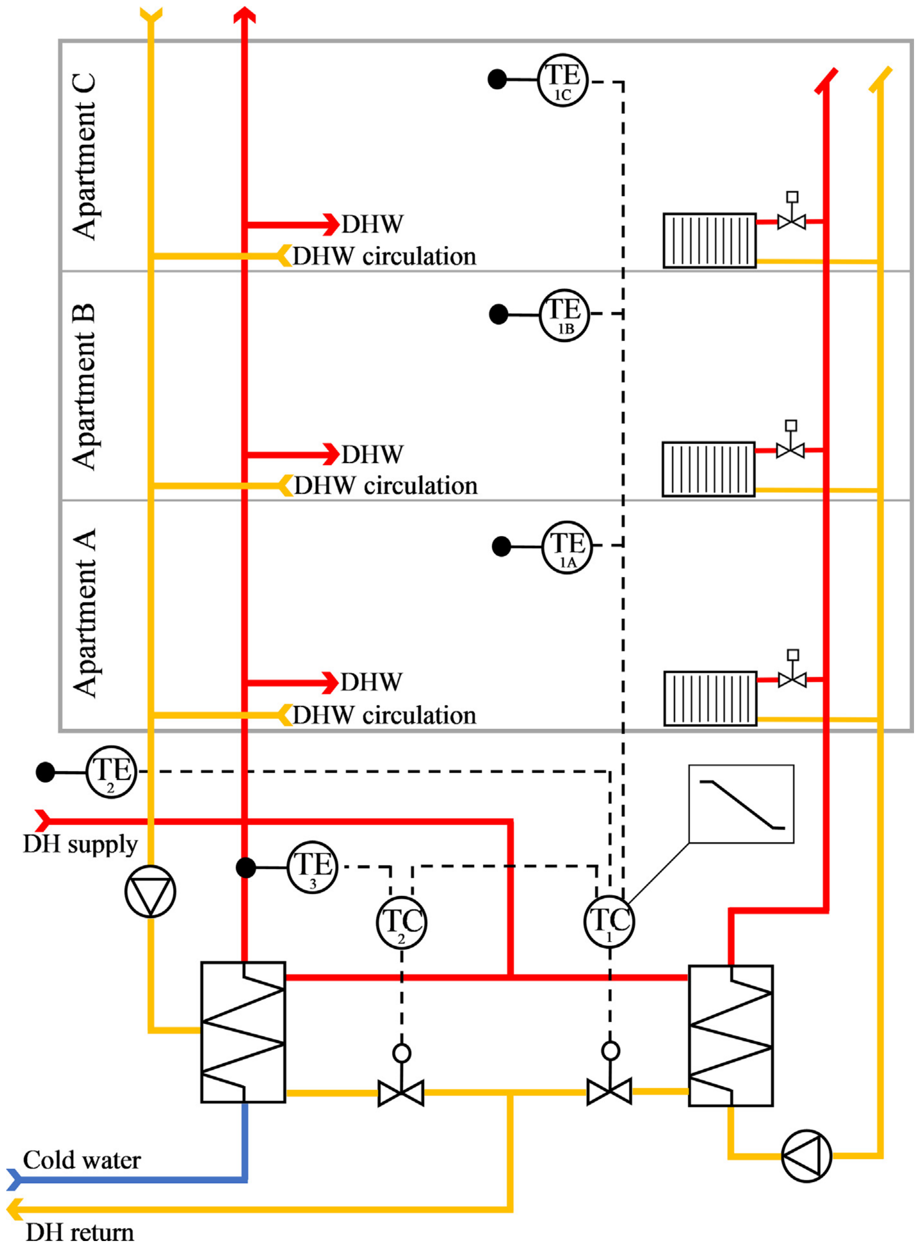

Fig. 5. The dynamic heating control system scheme.

These parameters were outdoor air (T_o) compensated 70/40/21 °C heating curve supply temperature (T_{HC}), the minimum air temperature among all zones (T_{min}), and the DHW distribution factor (DF_{DHW}). Fig. 6 represents the dynamic heating control algorithm flowchart.

Firstly, we used a second-order polynomial to define outdoor air compensated 70/40/21 °C heating curve with Eq. (1) describing the correlation between the HC supply temperature (T_{HC}, °C) and outdoor air temperature (T_o, °C).

$$T_{HC} = -0.0041T_o^2 - 1.0265T_o + 45.708 \tag{1}$$

Secondly, the space heating compensation temperature ($T_{SH,\ CT}$) was set as 5 °C, meaning that if the minimum indoor air temperature in any zone (T_{min}) drops below 19.5 °C, the SH supply temperature will be increased by 5 °C. Otherwise $T_{SH,\ CT}$ = 0.

Thirdly, we applied the DHW Distribution Factor (DF_{DHW}) depending on the hourly DHW consumption profile (see Fig. 2) to calculate the DHW compensation temperature ($T_{DHW,\ CT}$, °C) that reduces the SH supply temperature at increased DHW consumption based on Eq. (2). Stage one applies when the DF_{DHW} is below 0.5, and no temperature reduction occurs in the supply temperature at this stage. Stage 2 is specified when the DF_{DHW} fluctuates between 0.5 and 2.5. In this case, the supply temperature is descended 5 times the corresponding DF_{DHW}. Stage 3 is determined when the DF_{DHW} stays above 2.5. In this condition, SH supply temperature is reduced by a maximum value of 12.5 °C.

$$T_{DHW,CT} = \begin{cases} 0, DF_{DHW} < 0.5 \\ -5 * DF_{DHW}, 0.5 < DF_{DHW} < 2.5 \\ -12.5, DF_{DHW} > 2.5 \end{cases} \tag{2}$$

The final dynamic supply temperature ($T_{Dyn.\ sup.}$, °C) was defined as the summation of the HC supply temperature (T_{HC}, °C), space heating compensation temperature ($T_{SH,\ CT}$, °C), and DHW compensation temperature ($T_{DHW,\ CT}$, °C) reduction, as shown in Eq. (3).

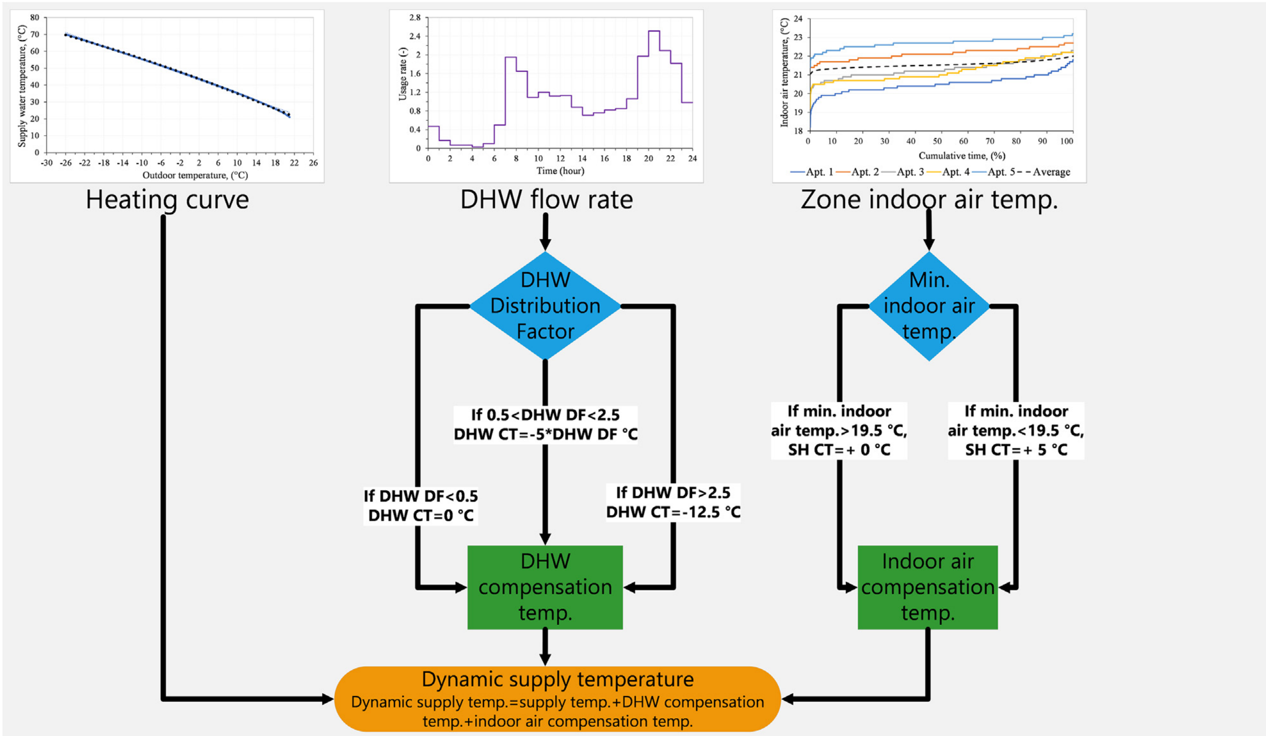

Fig. 6. The dynamic heating control algorithm flowchart.

$$T_{Dyn.\ sup.} = T_{HC} + T_{SH,\ CT} + T_{DHW,\ CT} \quad (3)$$

Fig. 7 illustrates the implementation of the developed heating control in IDA ICE. The outdoor air temperature sensor (1) data was used for HC supply water temperature Eq. (1) implemented in macro (3). The minimum apartment temperature among all apartments was detected via zone sensor (2) and summed together with (1) at the macro at (3), as it was explained in Eq. (2). At (4), the DHW control signal based on the DF_{DHW} was identified, and the $T_{DHW,\ CT}$ was adjusted according to get the optimal condition at (5). Finally, at (6), the DHW compensation temperature according to (4) and (5) was summed up with (3) and regulated the supply water temperature as explained in Eq. (3).

3.2. Model calibration and validation

Since some data, such as separately measured DHW consumption, ventilation airflow rate, and DHW circulation heat loss, were not directly available and were estimated from available measured data and design documentation, the first energy simulation results led to an inaccurate result called an uncalibrated energy balance. After input data parameter identification, the calibrated results closely matched the measured data. The conventional model calibration and results with 2018 data are discussed in detail in [21]. Table 2 shows the annual measured, uncalibrated, and calibrated energy balance breakdown. The uncalibrated DHW values were the building code defaults that were not used in the calibrated model for which real values were determined. The measured electricity data included tenant and facility electricity, simulated in IDA ICE as fans, pumps, appliances, and lighting.

To assess the simulation model's accuracy, the d and CV(RMSE) values were computed in different energy demand categories such as SH, DHW and total electricity. The corresponding d and CVRMSE values remained in the standard range (<15%), indicating the model validity and accuracy. The results are shown in Table 3.

The dynamic control model was calibrated against the average indoor air temperature measured. The measured average indoor air temperature was compared to the mean air temperature at the apartment level to determine the model validation and accuracy that resulted in d and the CVRMSE values of 0.53 and 1.99 %, respectively.

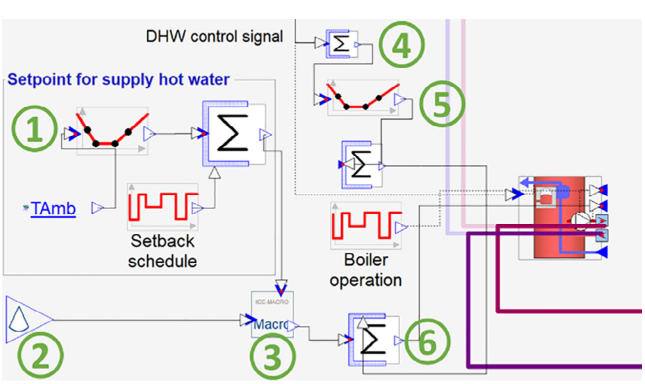

Fig. 7. The dynamic heating control system implemented in IDA ICE.

Table 2
The measured, uncalibrated, and calibrated energy balance in 2018.

Consumption	Energy, kWh/m^2		
	Measured	Uncalibrated	Calibrated
Space Heating (SH)	78.24	83.36	76.87
Domestic Hot Water (DHW)	29.92	35	29.63
DHW circulation heat losses	26.50	11.56	26.49
Fans and pumps	36.34	3.57	4.43
Appliances		22.03	24.32
Lighting		7.01	7.73
Total	**171.0**	**162.5**	**169.5**

Table 3
The d and CV(RMSE) values in three energy demand categories after the model calibration in 2018.

Energy demand	Index of agreement, d	CV(RMSE)
SH	0.997	9.75 %
DHW	0.673	3.36 %
Total Elec.	0.764	5.10 %

According to Table 2, the calibrated model's SH and DHW energy usage in 2018 was calculated to be 132.9 kWh/m2. As mentioned in section 2.2, the conventional model was first run with 2020 weather data to assess the impacts of the dynamic control algorithm on power reduction and energy use. This resulted in 113.9 kWh/m2 SH and DHW, that is 19 kWh/m2 less than in the calibrated model 2018, showing that either 2018 or 2020 weather data needs to be used for detailed comparison as the 2018 winter was significantly colder, Fig. 8. The heating period average outdoor temperature in 2018 and 2020 between October and April was 0.5 °C and 3.9 °C, respectively. Furthermore, the number of hours when the outdoor temperature was below 0 °C was 25.3% in 2018 and 6.5% in 2020.

3.3. Indoor air temperature evaluation and stability

The measured indoor air temperature in individual apartments in March 2020 is shown in Fig. 9. In 29% of the time in apartments 1, 4 and 3, the indoor air temperature was below 21 °C. The indoor air temperature in apartments 2, 5 and the average indoor air temperature among all apartments stayed above 21 °C. As discussed in section 2.5, the deviation of the indoor air temperature should be less than 6 % of yearly hours to satisfy the indoor air temperature criterion; therefore, 3 apartments out of 5 do not satisfy this criterion. For this reason, heating energy and power comparison was conducted with calibrated simulation model where conventional and dynamic control were applied with 2020 weather data.

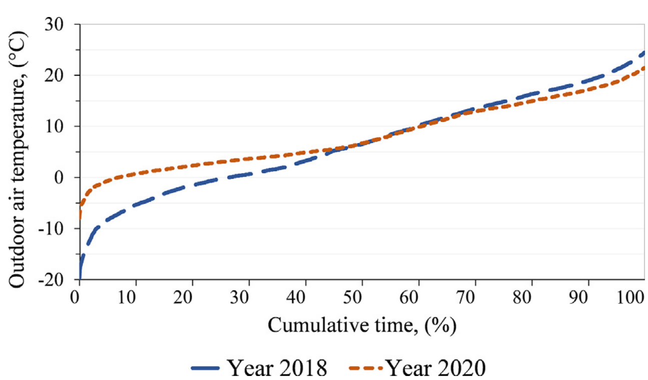

Fig. 8. The outdoor temperature duration curve in 2018 and 2020.

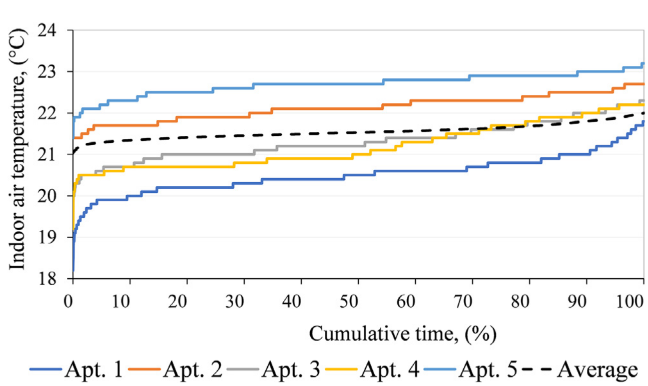

Fig. 9. The measured indoor air temperature between five apartments and the average of all apartments in March 2020.

Fig. 10 compares the measured indoor air temperature duration curve in March 2018 under the conventional control and March 2020 under the dynamic heating control system. March was the coldest month in both years; however, March 2018 was colder than 2020, not allowing to conduct a direct comparison of measured temperatures.

Simulated extract air temperature duration curves for 2020 full year weather data are compared in Fig. 11 for conventional and dynamic heating control. In the dynamic heating control system, the time below 21 °C was calculated as 0.2%, whereas in the conventional heating control system, there was no extract air temperature below 21 °C. It should be noted that in the heating energy and power comparison, this small difference gives an advantage to the dynamic control case.

This small temperature difference caused by dynamic control is further studied in Fig. 12, comparing the extract air temperature that describes the average indoor air temperature in the building during one week from March 01 to March 07, 2020. The dynamic heating control has caused extra temperature fluctuations, following the supply temperature reduction by the DHW compensation. Therefore, two temperature drops are visible in most of the days. Even though the average extract air temperatures were the same, 49.7% of the time, the extract air temperature with dynamic control remained lower than that with conventional control.

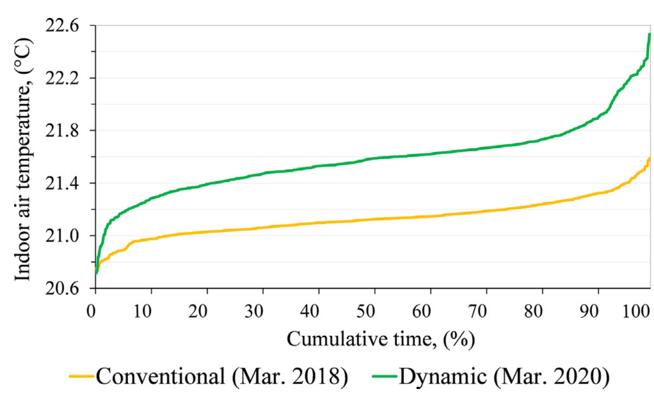

Fig. 10. Measured indoor air temperature in March 2018 with conventional control and in March 2020 with dynamic control.

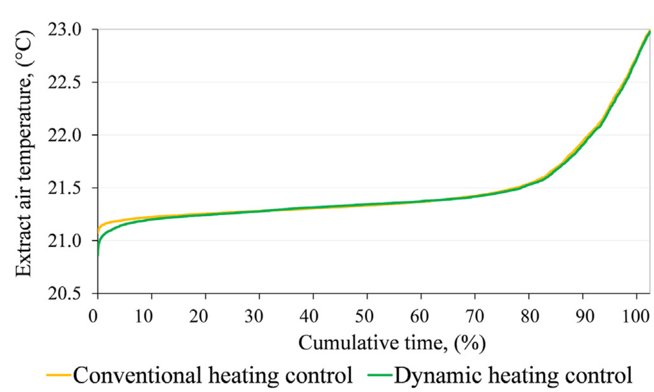

Fig. 11. Simulated extract air temperature for the full year 2020.

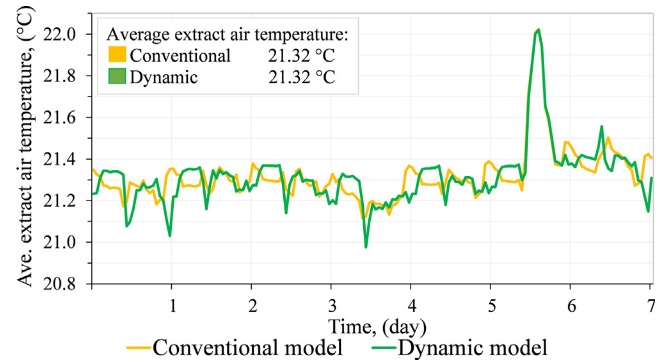

Fig. 12. Simulated extract air temperature in the conventional and dynamic heating control systems from March 01 to March 07, 2020.

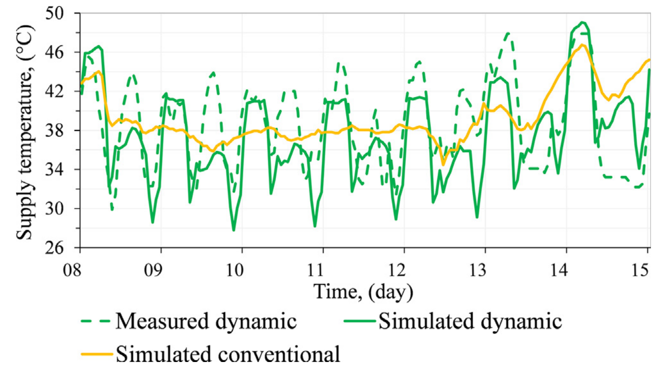

Fig. 13. The measured dynamic, simulated dynamic, and simulated conventional supply temperature from March 09 to 15, 2020.

Table 4
The mean indoor air temperature yearly hours' length of deviation below 21 °C in the conventional and dynamic heating control models.

Model		The mean indoor air temperature yearly hours' length of deviation below 21 °C, %	
		Apartment level	Building level
Conventional model, SP 21 °C	0.48	0.00	
Dynamic model	SP 20.5 °C	47.25	47.40
	SP 21 °C	0.52	0.02
	SP 21.5 °C	0.01	0.00

The amount of $T_{DHW,\ CT}$ was determined based on the value of the mean indoor air temperature yearly hours' length of deviation below 21 °C. The dynamic heating control model was tested with various DHW compensation temperatures from −2.5 °C to −15 °C (in 2.5 °C intervals) while the setpoint temperature remained the same (21 °C), and the corresponding mean indoor air temperature yearly hours' length of deviation below 21 °C was calculated individually. The maximum compensation of $T_{DHW,\ CT}$ was found to be −12.5 °C, which resulted in 0.52% of yearly hours below 21 °C, that is only slightly worse than 0.48% in the conventional control as shown in Table 4.

3.4. Dynamic control supply temperature

Fig. 13 depicts changes in measured dynamic, simulated dynamic, and simulated conventional supply temperature (70/40 heating curve) over a week in March 2020. The measured and simulated dynamic supply temperatures (dashed and solid green lines) indicated that they had the same frequency and amplitude; thus, the implemented dynamic control showed similar performance as the measured commercial one. It can be seen that the building was preheated twice a day while the DHW consumption was minimal. In contrast, the conventional heating control system operated with a more stable supply temperature, not depending on the DHW consumption fluctuations.

Fig. 14 compares the measured supply temperature in the conventional and dynamic heating control in the previous week from March 01 to 07, while the measured dynamic control did not operate in an optimal fashion. Response to two daily DHW peaks is visible, but regardless of DHW usage, the conventional supply temperature was lower during most of the time. A longer period is compared in Fig. 15, wherein 35% of days, the dynamic average supply temperature was higher than conventional. This indicates that the measured commercial dynamic control could be

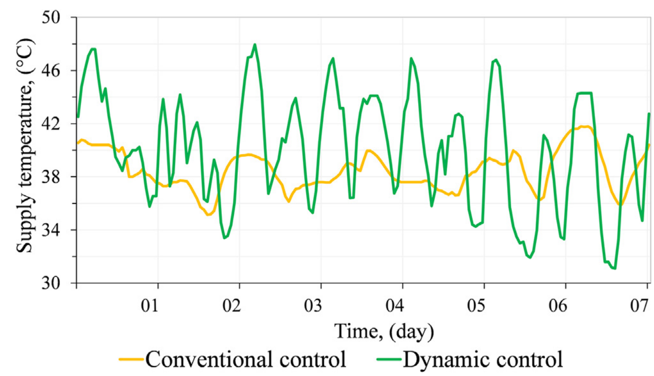

Fig. 14. Measured SH supply temperature in the conventional and dynamic heating control systems from March 01 to 07, 2020.

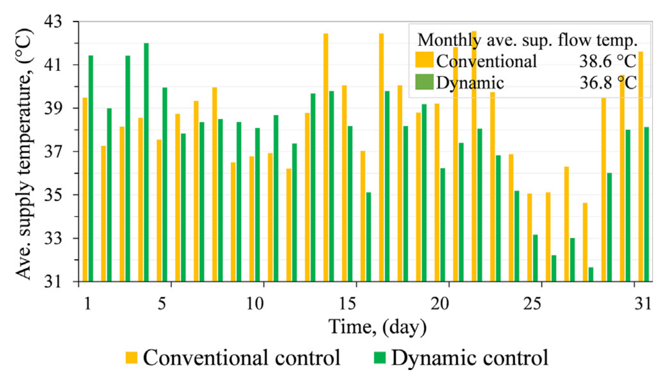

Fig. 15. Measured average daily SH supply temperature in conventional and dynamic heating control systems in March 2020.

improved. Despite the fact that the monthly average supply temperature of the dynamic control remained 1.8 °C lower than the conventional one, it may be suspected that the commercial dynamic heating control was not operated in its optimal fashion.

3.5. Dynamic control energy and power implications

The dynamic control equations were aimed to affect the SH supply temperature leading to reduced heating power and potentially to have some effect on heating energy. Fig. 15 shows the power and extract air fluctuations in the conventional and dynamic model in Feb (a) and May (b) 2020, representing winter and spring conditions. In Fig. 16(a), the conventional and dynamic control extract

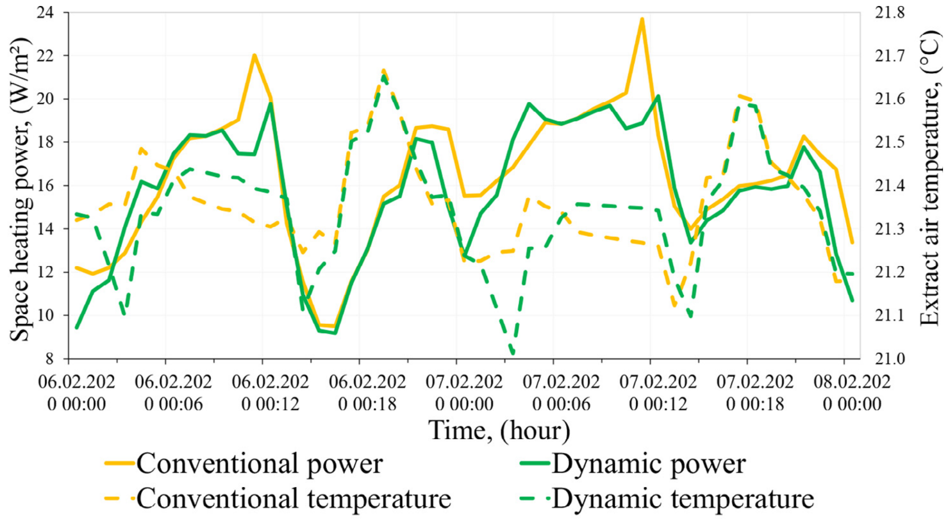

(a)

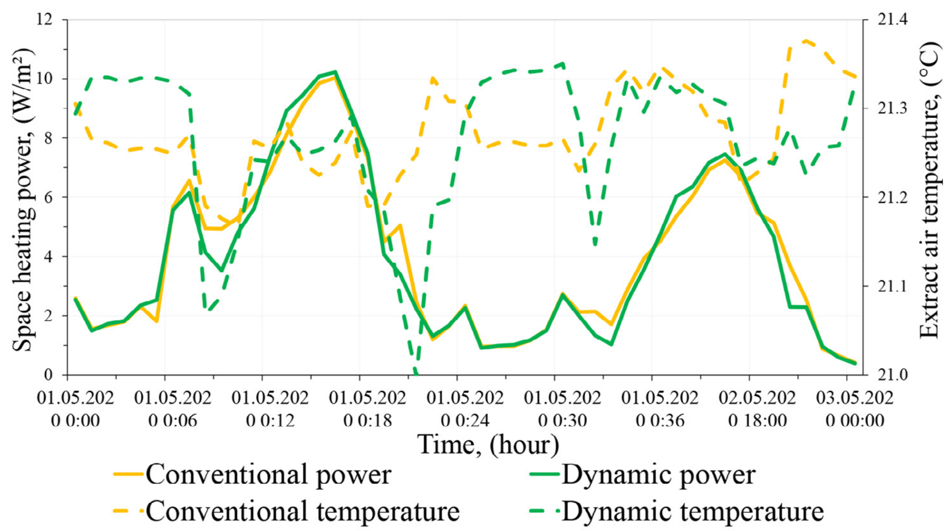

(b)

Fig. 16. Simulated SH power and extract air temperature in a) Feb 2020 and b) May 2020.

air temperature stayed above 21 °C, being on average 21.35 °C and 21.34 °C, respectively. The dynamic control SH heat exchanger peak power reduction is well visible, while the average SH heat exchanger power was slightly less in conventional control (16.33 W/m^2 vs 16.74 W/m^2).

In spring, Fig. 16(b), the average conventional and dynamic control extract air temperature was 21.27 °C and 21.26 °C, respectively, but the temperature drop pattern is visible. The conventional and dynamic control SH heat exchanger power were on average 4.06 W/m^2 and 3.95 W/m^2, respectively and did not show clear differences under this condition.

The total heating power includes the DHW and SH heating exchanger powers, which do not have maximums at the same time. The DHW heat exchanger power never reached zero; however, the SH heat exchanger power was zero in warm months. Fig. 17 compares the SH heat exchanger and total (DHW + SH) power duration curve in dynamic and conventional heating control for 2020. The conventional and dynamic SH heat exchanger power varied between 0 W/m^2 and 23.68 W/m^2, with average values of 6.47 W/m^2 and 6.29 W/m^2, respectively. Similarly, the conventional and dynamic total power laid between 3.07 W/m^2 and 32.84 W/m^2 with average values of 12.61 W/m^2 and 12.44 W/m^2, respectively, showing practically no difference in an average power but significant peak power reduction in the dynamic heating control system.

Fig. 18 compares the simulated energy use (a) and maximum powers (b) between the conventional control (setpoint temp. 21 °C) and dynamic control (setpoint temp. 21 °C, 21.5 °C, and 22 °C) while $T_{DHW,\,CT}$ was −12.5 °C. None of the dynamic equations influenced the DHW system, and therefore the DHW energy remained unchanged in both conventional and dynamic models. The SH and total energy use decreased by 3.2% and 1.6%, respec-

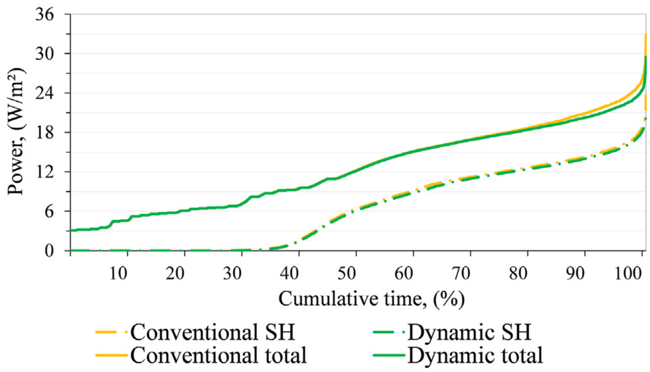

Fig. 17. Simulated SH and total power duration curve in conventional and dynamic heating control systems.

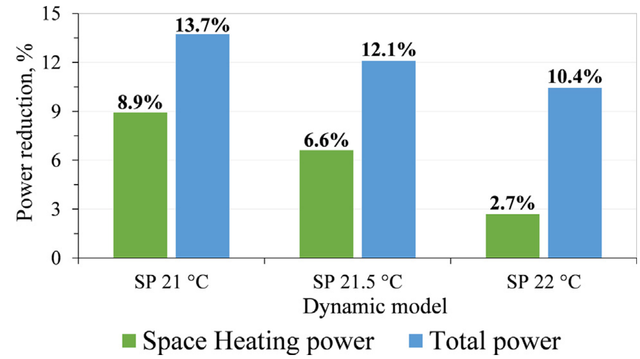

Fig. 19. The percentage of SH and total power reduction in the dynamic model in setpoint temperatures 21 °C, 21.5 °C and 22 °C.

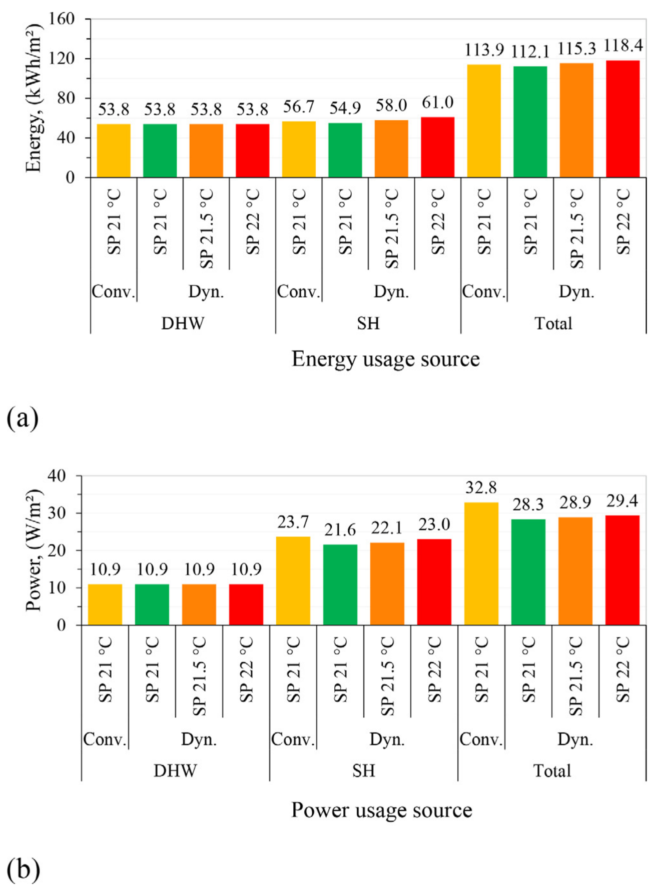

Fig. 18. The conventional and dynamic control comparison, a) energy use, b) heating power.

tively, which is explained by slightly lower indoor temperature in the case of dynamic control, as shown in Fig. 18(a). The corresponding dynamic heating control energy values with SP 21.5 °C already exceeded the conventional heating control energy use. Fig. 18(b) shows the maximum heating power in W/m^2. The DHW maximum power stayed constant since the DF_{DHW} remained unchanged in the conventional and dynamic models.

Fig. 19 presents the dynamic control model's SH and total power reduction considering different setpoint temperatures (21 °C, 21.5 °C and 22 °C). The dynamic heating control resulted in 8.9 % SH and 13.7% total maximum power reduction with SP 21 °C. Increasing the SP temperature resulted in slightly lower power reduction, which shows reasonably low sensitivity to the setpoint, indicating that for instance, settings by occupant will not eliminate the power reduction.

4. Conclusion

This study developed a dynamic central heating control algorithm and investigated the impacts on heating energy, power, and indoor air temperature in a typical old, not renovated, multi-family apartment building. The building was operated with conventional and dynamic heating control in 2018 and 2020. Both building simulation models were calibrated with the root mean square error of less than 10% against onsite measured data. By utilizing a DHW compensation differential, a new dynamic heating curve control algorithm was designed to reduce outdoor air compensated supply temperature during high use of DHW.

The results of the study allow us to draw the following conclusions:

Operation with the conventional heating curve in 2018 showed that the average measured indoor air temperature in 15% of all apartments was below 21 °C, indicating that it could be difficult to save heating energy by lowering the supply water temperature. Simulations with dropped heating curves revealed no energy-saving potential available because of decreased indoor air temperatures.

In 2020, the commercial heating control was implemented, and the building was preheated twice a day while the DHW consumption was minimal. The measured data were compared with a developed dynamic control simulation model, which operated according to the outdoor air compensated supply temperature, the minimum air temperature across all zones, and the DHW distribution factor. Simulated supply temperature followed a similar pattern to measured data of the commercial control; however, the latter did not always perform optimally since the dynamic average supply temperature was higher than the conventional one in 35% of the days of the measurement period.

Compared to the conventional heating control, the indoor air temperature yearly hours' length of deviation below 21 °C was changed from 0.48% to 0.52% in the dynamic control operation in 2020. Therefore, there was no need to increase setpoint temperature during the dynamic control. Nevertheless, the dynamic heating control caused unwanted indoor temperature fluctuations, resulting in 0.1–0.15 °C temperature drops compared to the conventional control and also slightly decreased average temperature.

The dynamic control had practically no effect on the space heating energy use, because a small reduction at the same temperature setpoint due to lower indoor air temperature turned to increased energy use at a higher setpoint. The dynamic control resulted in

8.9% space heating and 13.7% total heating power reduction. Considerable total power reduction is explained by DHW and SH power peaks at different times and shifting space heating power to the low DHW demand period when the building will be pre-heated. Thus, the results suggest that the dynamic control should be able to reduce the district heating connection power and fixed fee at least by 10%.

Generally, the developed dynamic control algorithm allowing to reduce the space heating supply temperature during DHW peaks, resulted in considerable power reduction without compromising indoor air temperature. As the proposed algorithm performs effectively in buildings with high DHW consumption, the control algorithm may be expected to be applied in residential and accommodation buildings with similar results. There is no application potential in other non-residential buildings with low DHW use. Furthermore, the dynamic algorithm delivers more significant results in heating systems with limited heating power, such as DH and heat pump systems. Therefore, it may not be feasible to implement the dynamic algorithm in heating systems with high power available, such as gas or other fuel boilers.

To continue the research on dynamic control, it would be worth in future studies to extend the analyses from the heating system to the primary side of the district heating, where it would be possible to apply a flow control in addition to the dynamic heating curve that was applied in this study. Investigating space heating and DHW heat exchanger's power reduction would be especially meaningful at design outdoor temperature that will determine the capacity for the district heating system.

Declaration of Competing Interest

The authors declare the following financial interests/personal relationships which may be considered as potential competing interests: Hatef Hajian reports financial support was provided by European Commission (Finest Twins, grant No. 856602). Hatef Hajian reports financial support was provided by Academy of Finland (grant 333365). Jarek Kurnitski reports financial support was provided by Estonian Ministry of Education and Research and European Regional Fund (grant 2014-2020.4.01.20-0289). Kaiser Ahmed reports financial support was provided by Estonian Centre of Excellence in Zero Energy and Resource Efficient Smart Buildings and Districts, ZEBE, grant 2014-2020.4.01.15-0016.

Acknowledgements

This research was supported by the European Commission (Finest Twins, grant No. 856602) by the Academy of Finland (grant 333365), by the Estonian Ministry of Education and Research and European Regional Fund (grant 2014-2020.4.01.20-0289) and by the Estonian Centre of Excellence in Zero Energy and Resource Efficient Smart Buildings and Districts, ZEBE, grant 2014-2020.4.01.15-0016 and the K.V. Lindholms Stiftelse foundation. We are thankful to Pekka Takki from Helen Ltd for his cooperation and sharing of energy info.

References

[1] H. Zhong, J. Wang, H. Jia, Y. Mu, S. Lv, Vector field-based support vector regression for building energy consumption prediction, *Appl. Energy*, 242, no. September 2018, pp. 403–414, 2019, doi: 10.1016/j.apenergy.2019.03.078.
[2] IEA & UNEP, "Global Status Report 2018 : Towards a zero-emission, efficient and resilient buildings and construction sector," *Global Status Report*, p. 325, 2018, [Online]. Available: http://www.ren21.net/status-of-renewables/global-status-report/.
[3] C. Filippín, S.F. Larsen, Energy efficiency in buildings, Energy Eff. Res. February (2009) 153–166, https://doi.org/10.1016/b978-0-12-822989-7.00016-0.
[4] Bosseboeuf et al., "Energy Efficiency Trends and Policies in the Household and Tertiary Sectors," no. June, p. 97, 2015.
[5] "Statistics Finland - Energy consumption in households 2018." https://www.stat.fi/til/asen/2018/asen_2018_2019-11-21_tie_001_en.html (accessed April 21, 2021).
[6] X. Cao, X. Dai, J. Liu, Building energy-consumption status worldwide and the state-of-the-art technologies for zero-energy buildings during the past decade, Energy Build. 128 (2016) 198–213, https://doi.org/10.1016/j.enbuild.2016.06.089.
[7] J. Randolph, G.M. Masters, Energy efficiency for buildings, Energy Sustain. 33 (1) (2018) 173–213, https://doi.org/10.5822/978-1-61091-821-3_6.
[8] "Statistics Finland, Buildings and free-time residences [e-publication, ISSN=1798-6796]," Helsinki, 2017.
[9] T. Vainio, M. Airaksinen, T. Vesanen, Space heating measurement in apartment buildings, p. 31, 2017, [Online]. Available: http://www.vttresearch.com/impact/publications).
[10] T. Benakopoulos, R. Salenbien, D. Vanhoudt, S. Svendsen, Improved control of radiator heating systems with thermostatic radiator valves without pre-setting function, *Energies (Basel)*, 12(17), 2019, doi: 10.3390/en12173215.
[11] M. Tunzi, D.S. Østergaard, S. Svendsen, R. Boukhanouf, E. Cooper, Method to investigate and plan the application of low temperature district heating to existing hydraulic radiator systems in existing buildings, Energy 113 (2016) 413–421, https://doi.org/10.1016/j.energy.2016.07.033.
[12] D.S. Østergaard, S. Svendsen, Experience from a practical test of low-temperature district heating for space heating in five Danish single-family houses from the 1930s, Energy 159 (2018) 569–578, https://doi.org/10.1016/j.energy.2018.06.142.
[13] T. Saloky, J. Pitel', Adaptive control of heating process with outdoor temperature compensation, *undefined*, 2005.
[14] B. Xu, A. Huang, L. Fu, H. Di, Simulation and analysis on control effectiveness of TRVs in district heating systems, Energy Build. 43 (5) (2011) 1169–1174, https://doi.org/10.1016/j.enbuild.2010.08.030.
[15] P.A. Elkhuizen, H.C. Peitsman, W.J. Wienk, A new design guideline for the heating and cooling curve in AHU units of HVAC systems, Build. Serv. Eng. Res. Technol. 24 (3) (2003) 191–202, https://doi.org/10.1191/0143624403bt071oa.
[16] P.A. Elkhuizen, J.E. Scholten, H.C. Peitsman, A. Kooijman, The effect of optimal tuning of heating-/ cooling curve in AHU of HVAC system in real practise, Icebo 1 (2004) 1–12.
[17] R. Rahif, D. Amaripadath, S. Attia, Review on time-integrated overheating evaluation methods for residential buildings in temperate climates of Europe, Energy Build. 252 (2021), https://doi.org/10.1016/j.enbuild.2021.111463 111463.
[18] A. Bruce-Konuah, R.V. Jones, A. Fuertes, L. Messi, A. Giretti, The role of thermostatic radiator valves for the control of space heating in UK social-rented households, Energy Build. 173 (2018) 206–220.
[19] C. Sun *et al.*, A dynamic control strategy of district heating substations based on online prediction and indoor temperature feedback, *Energy*, 235, 121228, 2021, doi: 10.1016/j.energy.2021.121228.
[20] A. Ionesi, M. Jradi, J. E. Thorsen, C. T. Veje, "Simulation of an adaptive heat curve for automatic optimization of district heating installation," *14th International Conference of IBPSA - Building Simulation 2015, BS 2015, Conference Proceedings*, pp. 2117–2124, 2015.
[21] H. Hajian, K. Ahmed, J. Kurnitski, J. Kurnitski, M. Thalfeldt, Estimation of energy-saving potential and indoor thermal comfort by the central control of the heating curve in old apartment buildings, E3S Web Conf. 246 (2021) 09002.
[22] "For Building Owners - Leanheat." https://leanheat.com/for-building-owners/ (accessed May 06, 2021).
[23] M. Kavgic, A. Summerfield, D. Mumovic, Z.M. Stevanovic, V. Turanjanin, Z.Z. Stevanovic, Characteristics of indoor temperatures over winter for Belgrade urban dwellings: indications of thermal comfort and space heating energy demand, Energy Build. 47 (2012) 506–514, https://doi.org/10.1016/j.enbuild.2011.12.027.
[24] S.K. Firth, K.J. Lomas, A.J. Wright, Targeting household energy-efficiency measures using sensitivity analysis, Build. Res. Inf. 38 (1) (2010) 25–41, https://doi.org/10.1080/09613210903236706.
[25] "Home - Finnish Meteorological Institute." https://en.ilmatieteenlaitos.fi/ (accessed April 30, 2021).
[26] "AIVC | Air Infiltration and Ventilation Centre." https://www.aivc.org/ (accessed April 30, 2021).
[27] ISO, "ISO 17772-1:2017 Energy performance of buildings — Indoor environmental quality — Part 1: Indoor environmental input parameters for the design and assessment of energy performance of buildings," *The International Organization for Standardization*, 2017. https://www.iso.org/standard/60498.html (accessed March 08, 2021).
[28] "National building code of Finland (Suomen säädöskokoelma)," Helsinki, 2017.
[29] K. Ahmed, P. Pylsy, J. Kurnitski, Hourly consumption profiles of domestic hot water for different occupant groups in dwellings, Sol. Energy 137 (2016) 516–530, https://doi.org/10.1016/j.solener.2016.08.033.
[30] Autodesk, "Revit _ BIM Software _ Autodesk Official Store," pp. 1–12, 2020, Accessed: March 07, 2021. [Online]. Available: https://www.autodesk.com/products/revit/overview?term=1-YEAR&support=null.
[31] J. L. M. H. N. Nakahara, H. Yoshida, M. Udagawa, Building simulation '99 : sixth international IBPSA conference, September 13-15, 1999, Kyoto, Japan : proceedings—Eindhoven University of Technology research portal, *Texas A&M Univ., Dep. of Architecture*, 1999. https://research.tue.nl/en/publications/

building-simulation-99-sixth-international-ibpsa-conference-septe (accessed March 07, 2021).
[32] EQUA Simulation AB, "IDA ICE - Simulation Software | EQUA," 2019. https://www.equa.se/en/ida-ice (accessed March 07, 2021).
[33] K. Tiilikainen, K. Outinen, Indoor climate and ventilation of buildings in Finland, 2017.
[34] Energy performance of buildings - Ventilation for buildings - Part 2: Interpretation of the requirements in EN 16798-1 - Indoor environmental input parameters for design and assessment of energy performance of buildings addressing indoor air quality, thermal environment, lighting and acoustics (Module M1-6).